PLANT SCIENCE

Gametophyte genome activation occurs at pollen mitosis I in maize

Brad Nelms[1]* and Virginia Walbot[2]

Flowering plants alternate between multicellular haploid (gametophyte) and diploid (sporophyte) generations. Pollen actively transcribes its haploid genome, providing phenotypic diversity even among pollen grains from a single plant. In this study, we used allele-specific RNA sequencing of single pollen precursors to follow the shift to haploid expression in maize pollen. We observed widespread biallelic expression for 11 days after meiosis, indicating that transcripts synthesized by the diploid sporophyte persist long into the haploid phase. Subsequently, there was a rapid and global conversion to monoallelic expression at pollen mitosis I, driven by active new transcription from the haploid genome. Genes showed evidence of increased purifying selection if they were expressed after (but not before) pollen mitosis I. This work establishes the timing during which haploid selection may act in pollen.

Plants do not make gametes directly after meiosis; instead, they form a multicellular haploid organism called the gametophyte. Although the size of the gametophyte is reduced in flowering plants (2 or 3 cells for male pollen and 4 to 15 cells for the female embryo sac), the haploid generation retains a high degree of independence. Gametophytes actively transcribe genes, with more than 60% of the genome expressed postmeiotically in pollen (*1*). Many genes are required during the haploid phase, as even modest chromosome deletions are not transmitted (*2*, *3*) and gametophytic mutants are routinely isolated in plant genetic screens (*4*). This widespread haploid expression exposes a large portion of the genome to natural selection in the gametophyte. Pollen, in particular, has a high capacity for selection because of large population sizes and intense competition during dispersal, pollen tube growth, and fertilization. Unsurprisingly, pollen selection has diverse consequences (*5*, *6*): It reduces inbreeding depression (*7*), increases offspring fitness (*8*), and contributes to sex chromosome evolution (*9*) and sex-specific differences in recombination rates (*10*). Pollen selection has further been employed in breeding programs to derive cold-tolerant crop varieties (*11*) and has been proposed as a key factor that drove the origin of flowering plants (*12*).

When does the haploid gametophyte genome take control from the genome of its diploid sporophyte parent? The haploid phase of pollen development is a complex and dynamic process that, in maize, lasts 20 days (*13*) (Fig. 1A)—roughly one-third of the time from seed to anthesis. There is no guarantee that gene products will be derived from the haploid genome immediately after meiosis. By comparison, the maternal genome controls most early events in animal postfertilization development, followed by a maternal-to-zygotic transition in which degradation of maternal products is coordinated with zygotic genome activation (*14*). Does an analogous parent-to-offspring transition occur in pollen? If plants provision some portion of pollen development with diploid-derived gene products, the timing and intensity of haploid selection would be constrained. We obtained allele-specific RNA sequencing (RNA-seq) data from single pollen precursors across 26 days of development, from the beginning of meiosis through pollen shed. These data allowed us to identify when expression from the haploid genome began and to follow its progress throughout time and on a gene-by-gene basis.

[1]Department of Plant Biology, University of Georgia, Athens, GA 30606, USA. [2]Department of Biology, Stanford University, Stanford, CA 94305, USA.
*Corresponding author. Email: nelms@uga.edu

Allele-specific RNA-seq of single pollen precursors

To test our ability to separate the contributions of parent (sporophyte) and offspring (gametophyte) to the transcriptome of single pollen precursors, we first isolated single diploid pollen mother cells (PMCs; i.e., cells poised to initiate meiosis) and haploid pollen grains from an F_1 hybrid between the A188 and B73 inbred maize lines. The PMC and mature pollen stages are separated by 26 days. We detected a mean of 364,003 transcripts per sample (unique molecular identifiers; see materials and methods). On average, 32.4% of transcripts could be unambiguously mapped to either the A188 or B73 parental alleles, hereafter referred to as genoinformative transcripts. At least one genoinformative transcript was detected for 16,730 genes (table S1).

In single PMCs, most genes were expressed from both alleles (Fig. 1B), as expected for diploid genome expression. By contrast, in mature pollen grains, genes were expressed almost exclusively from one allele (Fig. 1C). Although multiple biological mechanisms can produce monoallelic expression, two pieces of evidence confirm that pollen monoallelic expression reflects expression from the haploid genome. First, there was no bias toward either the A188 or B73 alleles (Fig. 1D), as would be predicted by parental imprinting or inbred-specific effects such as presence-absence variation. Second, extensive blocks of linked genes on chromosome arms were expressed from the same parental allele, with infrequent shifts to the alternate parental allele, as is characteristic of meiotic recombination (Fig. 1E and fig. S1). Using the allele-specific expression data, we infer an average of 1.36 crossovers per chromosome (fig. S2A), with more-frequent crossovers toward the telomeres (fig. S2B and table S2), in agreement with the established crossover frequency (*15*) and distribution (*16*) in maize. Thus, RNA-seq of single cells and pollen grains can distinguish expression originating from the diploid and haploid genomes.

Gene expression during pollen development

We next profiled 349 single pollen precursors collected from 67 staged anthers, with dense sampling from premeiotic interphase through mature pollen (Fig. 1F and table S2). To facilitate sample staging, precursors were collected from one anther for RNA-seq while the remaining two anthers from the same floret were fixed for microscopy. Reproducible correspondence was observed between gene expression and the microscopic stage (Fig. 1F). Because we will be comparing bi- and tricellular stages of pollen development with earlier unicellular stages, we collectively refer to these samples as single pollen precursors rather than single cells.

Gene expression did not change uniformly during development but rather showed periods of rapid change interspersed with periods of relative stasis. There was a large shift in gene expression during early meiotic prophase I (Fig. 1F and fig. S3), consistent with our previous description of an early prophase transcriptome rearrangement (*17*). This was followed by several smaller expression changes during the rest of prophase I, a comparably static transcriptome from metaphase I through the early unicellular microspore (UM) stage, and another large shift in expression between UMs and bicellular microspores (BMs). We found distinct temporal expression patterns for many gene categories (tables S4 and S5), including transcription factors, genes involved in meiotic recombination and synapsis (fig. S4), and phased small RNA precursors (fig. S5). This dataset provides a time course of gene expression throughout meiosis and pollen development.

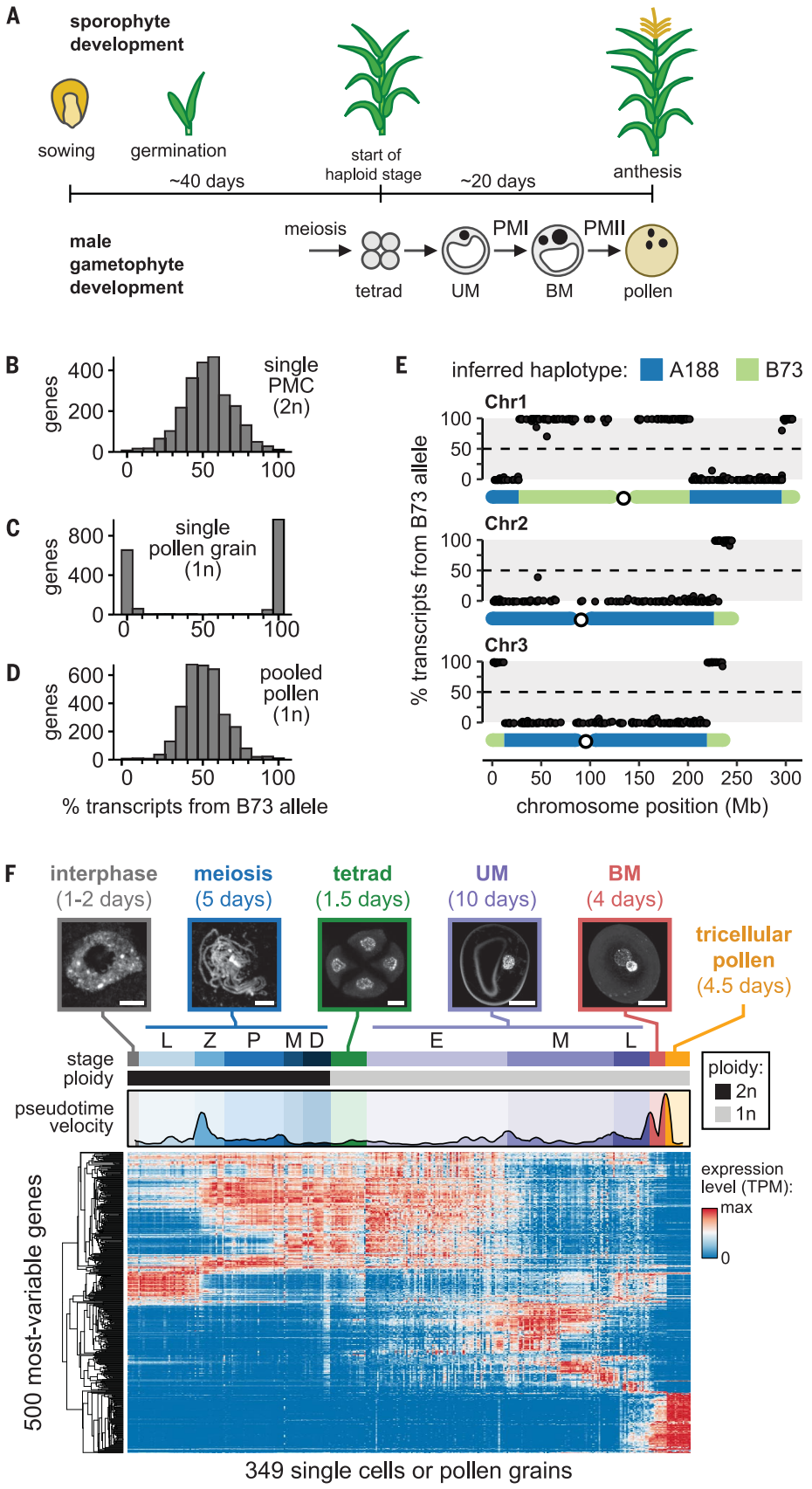

Fig. 1. Allele-specific RNA-seq of single pollen precursors. (**A**) Timeline of sporophyte and (male) gametophyte development. (**B** to **D**) Histogram of the fraction of transcripts matching the B73 allele for genes in (B) a single diploid PMC or (C) a single pollen grain, as well as (D) the average across pollen grains (computationally pooled data; *N* = 15 pollen grains). n, number of chromosomes. (**E**) Allelic bias of genes is correlated with their genomic location in a single pollen grain. The inferred haplotypes are shown below each graph. It is unclear whether the rare genes with apparent biallelic expression (non-0% or non-100% on the *y* axis) are the result of biological factors or technical noise; no genes were consistently biallelically expressed in multiple pollen grains (fig. S1 and 2C). In (B) to (E), all genes with at least 10 genoinformative transcripts are shown. (**F**) Single pollen precursors and pollen grains were isolated from maize anthers for RNA-seq. (Top) Exemplar microscopy images of DAPI (4′,6-diamidino-2-phenylindole)–stained material used for sample staging. (Middle) Pseudotime velocity, which quantifies the rate of expression change over time (*17*); peaks indicate periods of rapid gene expression change. (Bottom) Heatmap of gene expression for the 500 most-variable genes. Scale bars are 5 μm for interphase and meiosis and 20 μm for later stages. Substages of meiosis: L, leptotene; Z, zygotene; P, pachytene; M, meiosis I division; D, dyad. UM substages: E, early; M, middle; L, late.

Timing and extent of haploid expression

To follow the shift from diploid to haploid expression, we first compared the proportion of genes with biallelic and monoallelic expression in single precursors at each stage (Fig. 2A). Gene expression was categorized as monoallelic if >80% of transcripts were from a single allele and as biallelic otherwise. We observed biallelic expression for the majority of genes during meiosis I (median of 83.5% biallelic genes per cell; Fig. 2A) while the cells were still diploid. Cells at the haploid tetrad and UM stages displayed a similar level of biallelic expression, with a median of 82.5% of genes with biallelic expression per cell (interquartile range: 79.6 to 84.5%). Thus, premeiotic (biallelic) transcripts persist until the end of the UM stage, 11 days after meiosis. Subsequently, a rapid conversion to monoallelic expression occurred around the time of pollen mitosis I (PMI), with a median of 99.1 and 99.5% of genes with monoallelic expression in BMs and pollen grains, respectively. Linked genes were consistently expressed from the same allele in BMs and pollen but not in earlier stages (Fig. 2A, right, and fig. S6), a characteristic sign of haploid genome expression. Thus, the haploid microspore is provisioned with sporophytic transcripts, followed by a sharp transition to gametophytic expression around PMI.

Most genes had biallelic expression through PMI, but does a gene cohort exist with earlier expression from the haploid genome? To answer this, we needed to distinguish haploid expression from other causes of monoallelic expression for individual genes. One distinctive characteristic of haploid expression is that it does not produce any bias toward a specific allele; haploid-expressed transcripts will match the A188 allele in some precursors but the B73 allele in others, depending on the precursor haplotype (Fig. 2B and fig. S7). By contrast, most other causes of monoallelic expression result in a consistent skew toward one allele. For instance, in diploid meiotic cells 5.5% of genes were expressed monoallelically (>80% of transcripts from the most-abundant allele); however, such genes were consistently biased toward either the B73 or the A188 allele, so their expression can be distinguished from haploid expression (Fig. 2C). In UMs, 90.0% of genes had biallelic expression and only 0.1% had monoallelic expression (Fig. 2D and fig. S8; the remaining 9.9% were B73- or A188-biased). In the following stage (BMs), the reverse was true: 0.3% of genes had biallelic expression and 93.3% of genes had monoallelic expression. Thus, the shift to haploid expression is largely all-or-none: We found no evidence for genes that are expressed from the haploid genome before PMI or, conversely, that persist as biallelicly expressed transcripts beyond PMI. There may be early haploid-expressed genes that we did not sample in this study, as only 1068 genes had a sufficient number of genoinformative transcripts in the UM stage to infer haploid expression; however, any such genes would be rare exceptions or genes with a consistently low level of expression.

Conservation of gametophyte-expressed genes

In many species, genes expressed in mature pollen show evidence for increased selection (both purifying and adaptive) compared with those in the genomic background (*18*, *19*). One proposed explanation is that selection may be more efficient on the haploid generation (*18*, *19*). Because our data show that the haploid genome becomes active primarily after PMI—midway through pollen development—we asked whether there were differences in the average rate of nonsynonymous to synonymous substitutions (d_n/d_s) in genes expressed at different times in pollen development. We focused on genes with moderate or greater expression at each stage [≥100 transcripts per million (TPM)] because there was a nonmonotonic relationship between expression level and d_n/d_s at low levels of expression (fig. S9), complicating the interpretation for low-abundance transcripts. Genes expressed at ≥100 TPM after meiosis but not after PMI (i.e., genes expressed in the tetrad or UM stages but not later) showed a similar distribution of d_n/d_s compared with those in the genomic background (Fig. 3A and fig. S9). By contrast, genes expressed after PMI had a 30.7% lower median d_n/d_s, consistent with purifying selection acting in the haploid gametophyte. This stage-dependent change in d_n/d_s may be explained by the provisioning of haploid pollen precursors with diploid transcripts, eliminating heritable phenotypic variation until after PMI.

We next estimated the fraction of genes expressed in the diploid sporophyte that might be subject to haploid selection in pollen. To identify sporophyte-expressed genes, we obtained expression data from whole seedlings (roots and shoots), defining sporophytic genes as those expressed in either seedlings or diploid pollen precursors. Consistent with prior results (*1*, *20*), we found that a large fraction of the genome is expressed during both diploid and haploid stages: 87.3% of genes had detectable transcripts in both the sporophyte and gametophyte (Fig. 3B), and 54.0% were expressed at ≥100 TPM in both (Fig. 3C). Of these, a substantial portion were expressed after PMI and thus potentially subject to haploid selection (Fig. 3, B and C); this subset had a significantly lower median d_n/d_s (Fig. 3D). The haploid expression of these genes likely contributes to lowering the genetic load in diploid plants.

Widespread gametophyte genome activation at PMI

What is the contribution of new transcription versus transcript turnover to the shift to haploid expression? RNA dynamics usually cannot be inferred from steady-state transcript levels alone, because opposing changes in the rates of RNA synthesis and degradation can produce similar effects on transcript abundance. However, our data provide a way to separate synthesis from degradation, because during the haploid phase any new transcription can come from only one allele. We find that the mean number of transcripts per precursor changed substantially during pollen development (Fig. 4A), suggesting large differences in the relative rate of new synthesis versus that of degradation between stages. The number of transcripts per cell decreased steadily from the peak during early meiosis to the minimum at the UM stage. This was followed by a sharp, 7.5-fold increase in the total number of transcripts per precursor between late UMs and BMs (95% confidence interval = 3.0- to 14.2-fold; bootstrap test), indicating that substantial new transcription activity may drive the shift to monoallelic expression during this period. Indeed, 7361 genes had at least a twofold increase in absolute transcript abundance between late UMs and BMs (Fig. 4B), and this increase was attributable to the more-abundant (haploid) allele (Fig. 4C). By contrast, the less-abundant allele remained relatively constant between UMs and BMs (median fold change of 0.02; Fig. 4D). This suggests that premeiotic (biallelic) transcripts persist into the BM stage for many genes but that a large increase in new transcription overtakes preexisting transcript levels to produce a net shift toward monoallelic expression. Thus, the transition to haploid expression is driven by new transcription and gametophyte genome activation, with degradation of sporophytic transcripts playing a relatively minor role at the transition.

De novo motif analysis identified the RY repeat (CATGCA[TG]) as significantly enriched in the promoters of the 200 most up-regulated genes during PMI, with 35 of 200 promoters (17.5%) having a perfect match to the full RY repeat (6.1-fold enrichment; $P = 7.1 \times 10^{-15}$, Fisher's exact test) and 72 promoters (36%) containing the minimal CATGCA motif (2.4-fold enrichment; $P = 6.2 \times 10^{-9}$, Fisher's exact test). The RY repeat is the binding site for three paralogous transcription factors (ABI3, FUS3, and LEC2) that regulate embryogenesis in *Arabidopsis* (*21*). Although the RY repeat has no known function in pollen development, conserved RY repeats have been observed in the pollen-specific β-expansin genes (*22*). This sequence may serve as the binding site for a transcription factor that contributes to gametophyte genome activation.

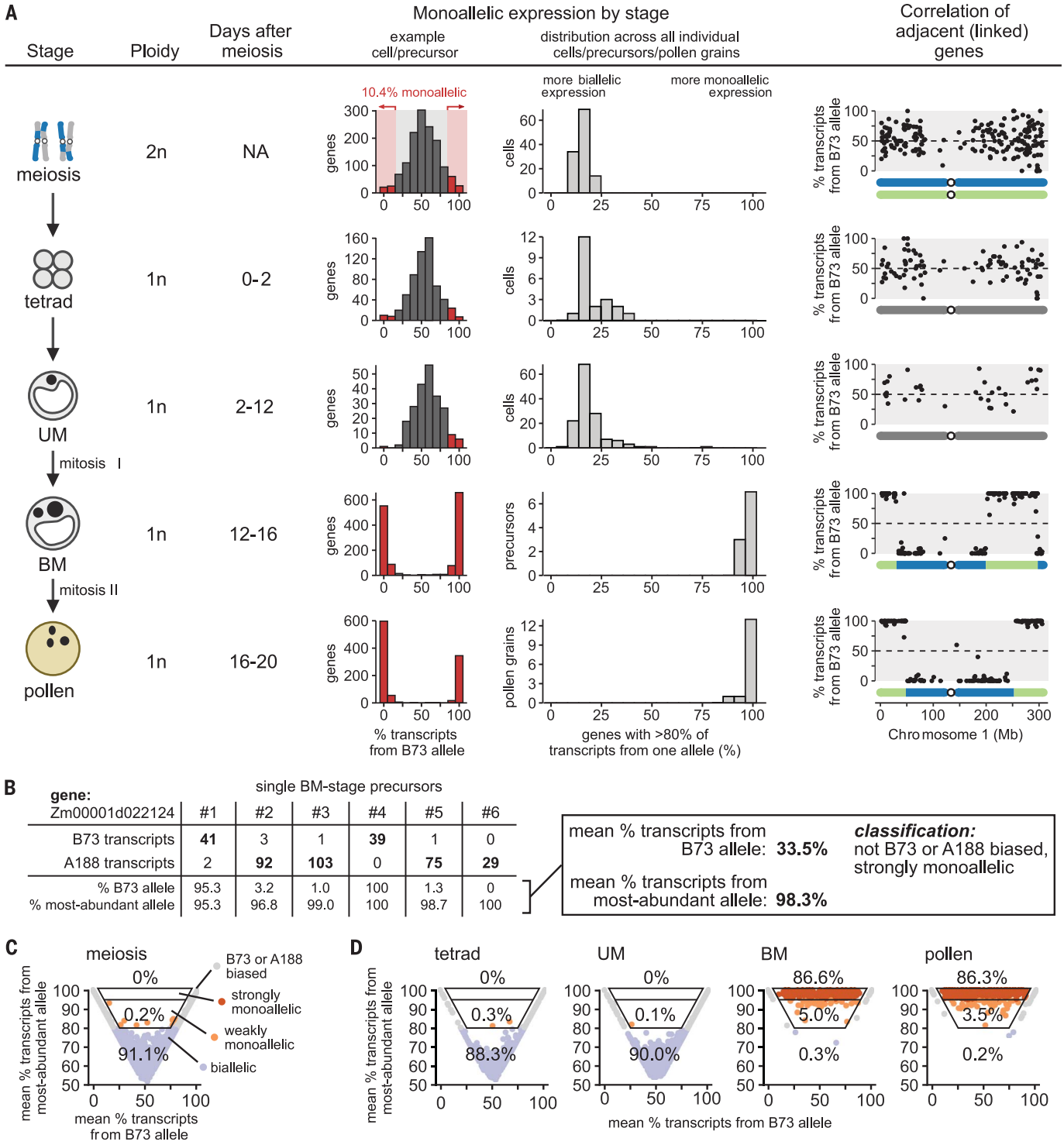

Fig. 2. Timing of haploid expression during pollen development. (**A**) Table showing the proportion of monoallelic expression for each stage in pollen development. Column three: mean number of days after meiosis when each stage begins and ends (*13*). NA, not applicable. Column four: histogram of genes, showing the fraction of transcripts matching the B73 allele in a representative precursor. Column five: histogram of precursors, showing the percentage of monoallelic genes in all precursors at a given stage. Column six: percentage of transcripts matching the B73 allele for each gene, by location on chromosome 1. (**B**) Expression data from individual BMs for *Zm00001d022124*, a representative haploid-expressed gene. This gene falls in the "strongly monoallelic" category in (C). Only BMs with at least 10 genoinformative transcripts are shown; see fig. S7 for the complete data for this and other example genes. (**C** and **D**) Scatter plots showing the mean percentage of transcripts matching the B73 allele versus the mean percentage matching the most-abundant allele within a precursor for each gene, by stage. The two boxed regions near the top of the plot highlight genes with strong monoallelic expression (red dots; >95% from the most-abundant allele) and weak monoallelic expression (orange dots; 80 to 95% from the most-abundant allele), excluding genes with a consistent bias toward a specific parental allele (gray dots).

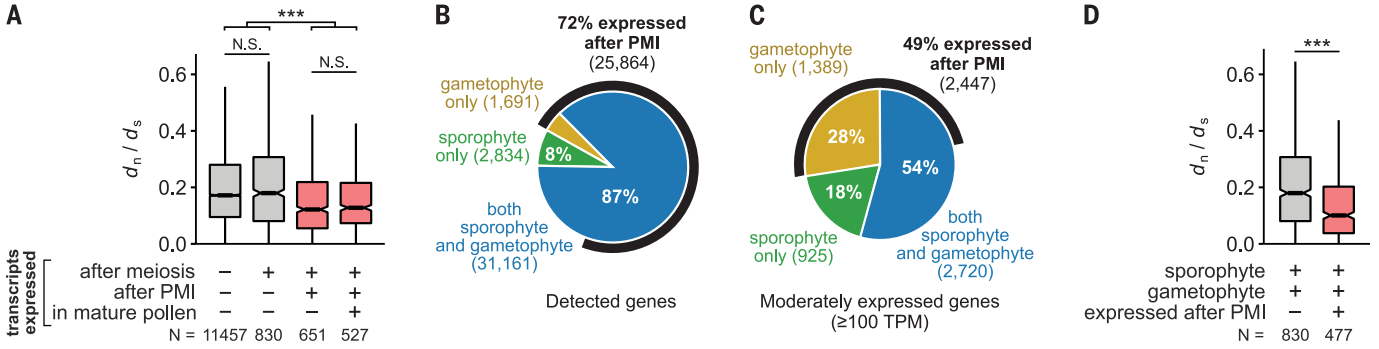

Fig. 3. Conservation of gametophyte-expressed genes. (**A**) Ratio of the number of nonsynonymous substitutions per nonsynonymous site (d_n) to the number of synonymous substitutions per synonymous site (d_s) for genes expressed at different times in pollen development. Categories of genes expressed after PMI are shaded red. N, number of genes. (**B** and **C**) Proportion of genes detected (B) or expressed at ≥100 TPM (C) in the sporophyte, gametophyte, or both. The number of genes expressed after PMI is also indicated. (**D**) d_n/d_s for genes expressed in both the gametophyte and sporophyte stages, separated on the basis of whether they were expressed after PMI. For (A) and (D), only genes expressed at ≥100 TPM were considered. Box plots show the median (horizontal line), interquartile range (IQR; shaded area), and whiskers extending up to 1.5 times the IQR. Gene categories expressed after PMI are shaded red. ***$P < 0.001$; Wilcoxon test adjusted for multiple hypothesis testing with Holm's method. N.S., not significant.

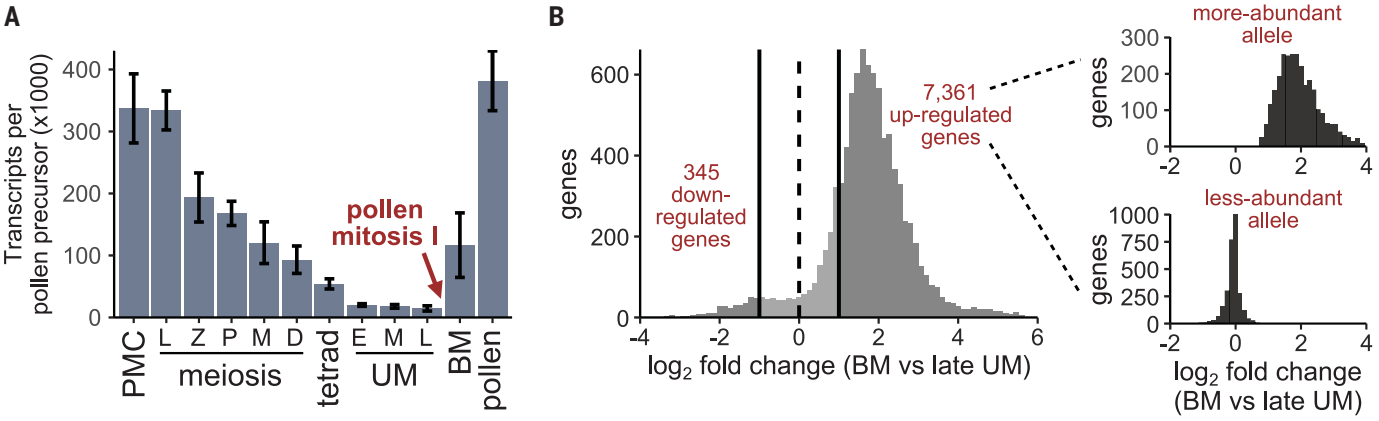

Fig. 4. Widespread gametophyte genome activation at PMI. (**A**) Total transcripts detected per pollen precursor, by stage. Shown are trimmed means (trim = 0.2) ± SE, estimated by bootstrapping. (**B**) (Left) Log_2 fold change in absolute transcript abundance between the late UM and BM stages for genes with a mean expression level of at least one transcript per precursor. Solid black lines separate genes up- or down-regulated by twofold or more. (Right) Log_2 fold change in transcript abundance for transcripts mapping to the more- and less-abundant alleles (top and bottom, respectively), showing only genes with a twofold or greater increase in overall transcript abundance. Up-regulated genes show an increase in transcript levels for the more-abundant (haploid) allele only.

Gene regulation before PMI

Before PMI, there appeared to be very little new transcription from the haploid genome, as evident in the continued biallelic status of most transcripts (Fig. 2). There were, however, clear changes in relative transcript abundance entering the mid- and late-UM stages (Fig. 1F and tables S4 and S5). To understand how the transcriptome might change in the absence of new transcription, we examined the absolute transcript abundance attributable to each allele for UM-expressed genes. Most genes showed biallelic transcript loss in UMs, ranging from rapid loss (fig. S11A) to slower degradation over time (fig. S11B). Thus, differences in mRNA half-life explain some expression changes during the UM stage. Many genes also had a biallelic increase in transcripts within UMs (fig. S11, C and D). What could cause a biallelic transcript increase in a haploid cell? One possibility is that these transcripts were synthesized premeiotically but then stored and not processed until later. Our sequencing libraries enrich for polyadenylated RNA and consequently do not detect stored RNAs with a short or missing polyadenylate tail. The storage of unprocessed RNAs has been described in other pathways, such as seed development (*23*), and would provide a mechanism for regulation of gene expression during the UM stage without transcription from the haploid genome. Collectively, our data show that the UM transcriptome is not static despite the lack of new transcription.

Discussion

Our study shows that diploid-derived transcripts persist long into the haploid phase of maize pollen development, followed by a rapid transition to monoallelic expression around PMI. We propose to call this the sporophyte-to-gametophyte transition (SGT), in analogy to the maternal-to-zygote transition (MZT), as both represent a shift from parent to offspring expression between generations. The widespread provisioning of the UM with sporophytic transcripts indicates a substantial parental investment in the developing gametophyte and implies that most cellular processes are under sporophytic control for the first half of pollen development.

Why might the SGT be delayed until PMI? One explanation is that PMI sets up the gametophyte germline (generative cell) and soma (vegetative cell). Active transcription is associated with an increased mutation rate (*24*); therefore, limiting transcription during the UM stage might reduce transcription-coupled DNA damage and accessibility of the genome to transposons. After PMI, the somatic vegetative cell is far more transcriptionally active than the generative cell (*25*) and could accommodate transcription without an associated risk to the germline. It will be important to establish whether SGT timing varies between species and between male and female gametophytes. Is PMI a conserved moment of gametophyte genome activation? Or does the SGT occur at different times in distinct plant lineages?

The substantial increase in new transcripts around PMI suggests that the SGT is driven by gametophyte genome activation resulting in new transcription, although the mechanisms of this activation are unknown. It is unlikely that the mitotic division itself is required to activate transcription, as vegetative cell-like development continues even when PMI is blocked (*26*–*28*), and several gametophytic mutants have been isolated that disrupt PMI (*4*). Our working hypothesis is that the SGT begins immediately before PMI rather than during this stage. Many substantial changes have been observed around PMI, including broad shifts in protein and RNA composition (*29*), transposon activity [in *Arabidopsis* (*30*)], and histone modifications (*31*). There is much to learn about how these pathways are coordinated to establish the independence of the gametophyte generation.

The scope of haploid selection in predominantly diploid organisms has long been debated (*6*). Plants are generally accepted to experience greater haploid selection than animals, in part because they require many genes to complete the haploid phase (*2*–*4*). By contrast, fully enucleate animal sperm are viable and can fertilize an egg (*6*). This distinction between kingdoms may be more nuanced than previously thought: Many genes have haploid-biased expression in mammalian sperm (*32*), which suggests that animal sperm may have a greater amount of heritable phenotypic variation than often assumed. Our results demonstrate an absence of haploid transcript accumulation for half of the haploid phase in maize pollen, limiting the time period that haploid selection may act in the male plant gametophyte. The ability to measure allele-specific expression directly in haploid gametes and gametophytes will provide needed clarity on this short but important life-cycle stage.

REFERENCES AND NOTES

1. S. D. Tanksley, D. Zamir, C. M. Rick, *Science* **213**, 453–455 (1981).
2. G. S. Khush, C. M. Rick, *Genetica* **38**, 74–94 (1967).
3. B. Kindiger, J. B. Beckett, E. H. Coe Jr., *Genome* **34**, 579–594 (1991).
4. L. C. Boavida *et al*., *Genetics* **181**, 1369–1385 (2009).
5. F. E. G. Beaudry, J. L. Rifkin, S. C. H. Barrett, S. I. Wright, *Plant Commun.* **1**, 100115 (2020).
6. S. Immler, *Annu. Rev. Ecol. Evol. Syst.* **50**, 219–236 (2019).
7. W. S. Armbruster, D. Gobeille Rogers, *Am. J. Bot.* **91**, 1939–1943 (2004).
8. D. L. Mulcahy, *Nature* **249**, 491–493 (1974).
9. G. Sandler, F. E. G. Beaudry, S. C. H. Barrett, S. I. Wright, *Evol. Lett.* **2**, 368–377 (2018).
10. T. Lenormand, J. Dutheil, *PLOS Biol.* **3**, e63 (2005).
11. H. J. Clarke, T. N. Khan, K. H. M. Siddique, *Euphytica* **139**, 65–74 (2004).
12. D. L. Mulcahy, *Science* **206**, 20–23 (1979).
13. S. Hsu, Y. Huang, P. Peterson, *Maydica* **33**, 77–98 (1988).
14. K. N. Schulz, M. M. Harrison, *Nat. Rev. Genet.* **20**, 221–234 (2019).
15. G. K. Sidhu *et al*., *Proc. Natl. Acad. Sci. U.S.A.* **112**, 15982–15987 (2015).
16. P. M. A. Kianian *et al*., *Nat. Commun.* **9**, 2370 (2018).
17. B. Nelms, V. Walbot, *Science* **364**, 52–56 (2019).
18. T. I. Gossmann, M. W. Schmid, U. Grossniklaus, K. J. Schmid, *Mol. Biol. Evol.* **31**, 574–583 (2014).
19. R. Arunkumar, E. B. Josephs, R. J. Williamson, S. I. Wright, *Mol. Biol. Evol.* **30**, 2475–2486 (2013).
20. A. M. Chettoor *et al*., *Genome Biol.* **15**, 414 (2014).
21. H. Jia, M. Suzuki, D. R. McCarty, *WIREs Dev. Biol.* **3**, 135–145 (2014).
22. E. R. Valdivia, J. Sampedro, J. C. Lamb, S. Chopra, D. J. Cosgrove, *Plant Physiol.* **143**, 1269–1281 (2007).
23. B. Harris, L. Dure 3rd, *Biochemistry* **17**, 3250–3256 (1978).
24. N. Kim, S. Jinks-Robertson, *Nat. Rev. Genet.* **13**, 204–214 (2012).
25. S. McCormick, *Plant Cell* **5**, 1265–1275 (1993).
26. C. Eady, K. Lindsey, D. Twell, *Plant Cell* **7**, 65–74 (1995).
27. J. Zhang *et al*., *Nat. Plants* **3**, 17079 (2017).
28. B. Glöckle *et al*., *Development* **145**, dev152645 (2018).
29. P. A. Bedinger, M. D. Edgerton, *Plant Physiol.* **92**, 474–479 (1990).
30. R. K. Slotkin *et al*., *Cell* **136**, 461–472 (2009).
31. M. Borg, F. Berger, *Plant J.* **83**, 177–188 (2015).
32. K. Bhutani *et al*., *Science* **371**, eabb1723 (2021).

ACKNOWLEDGMENTS

We thank J. Ross-Ibarra and E. Josephs for helpful discussions, J. Dinneny for use of the SP8 confocal microscope, and S. Liu for providing the A188 genome sequence ahead of publication. **Funding:** This work was supported by National Science Foundation award 17540974. B.N. was supported by an NSF PGRP postdoctoral fellowship. **Author contributions:** B.N. and V.W. designed experiments, discussed results, and wrote the manuscript. B.N. conceived the project, performed experiments, and conducted data analysis. **Competing interests:** The authors declare no competing interests. **Data and materials availability:** Sequencing data and mapped allele-specific transcript counts are available at the NCBI Gene Expression Omnibus (accession no. GSE175916). All other data required to evaluate the conclusions are in the main paper or the supplementary materials.

SUPPLEMENTARY MATERIALS

science.org/doi/10.1126/science.abl7392
Materials and Methods
Figs. S1 to S12
Tables S1 to S6
References (*33*–*49*)
MDAR Reproducibility Checklist

View/request a protocol for this paper from *Bio-protocol*.

5 August 2021; accepted 9 December 2021
10.1126/science.abl7392